Fig. 3 Photocurrent-wavelength spectra for GaAs/ $GaAs_{0.5}P_{0.5}$ SLS. *a* And *b* represent two different regions of the SLS wafer. Solid lines, theoretical fits to seven gaussian lines with equal linewidths.

to the outer surface of the SLS, where the layer distortions and strains are greater (see Fig. 1), and hence suffer faster $e^- - h^+$ recombination rates.

The quantum efficiencies exhibited by the present sample are consistent with electron diffusion lengths of the order of 0.05 μm. As expected, this is much lower than the values of 1-2 μm for bulk GaAs or for diffusion parallel to the superlattice layers[12]. The lower values for the perpendicular direction are caused by inhibition of charge transfer by the $GaAs_{0.5}P_{0.5}$ barriers. Significant penetration through the relatively thick barriers could be attributed to enhanced tunnelling created by strain-induced defect states in the barrier. Another possibility is that thermionic emission processes may have a role. Further work is required to understand these results more completely.

The good resolution of the photocurrent spectra even at room temperature is surprising; optical absorption and emission experiments are usually done at low temperatures to produce good spectral resolution. Further experiments as a function of SL composition, well and barrier dimensions, and temperature are in progress.

The ability of MQWs and SLs to absorb light at discrete quantum levels and permit charge transfer from these levels provides a potential mechanism for achieving the high theoretical thermodynamic conversion efficiencies predicted for hot carrier injection processes[13]. This is because carrier relaxation to the semiconductor band edges (defined for bulk material), with its attendant thermal loss, is inhibited by the presence of discrete energy levels with relatively large separation.

1. Esaki, L. & Chang, L. L. *Phys. Rev. Lett.* **33**, 495-498 (1974).
2. Dingle, R., Gossard, A. C. & Wiegmann, W. *Phys. Rev. Lett.* **34**, 1327-1330 (1975).
3. Dingle, R. *Festkörperprobleme* **15**, 21-48 (1975).
4. Ploog, K. & Döhler, G. H. *Adv. Phys.* **32**, 285-359 (1983).
5. Osbourn, G. C. *J. Vac. Sci. Technol.* **21**, 379-382 (1983).
6. Gourley, P. L. & Biefeld, R. M. *Appl. Phys. Lett.* **45**, 749-751 (1984).
7. Dohler, G. H. *Scient. Am.* **249**, 144-151 (1984).
8. Brus, L. E. *J. chem. Phys.* **80**, 4403-4409 (1984).
9. Rossetti, R., Ellison, J. L., Gibson, J. M. & Brus, L. E. *J. chem. Phys.* **80**, 4464-4469 (1984).
10. Nozik, A. J., Williams, F., Nenadović, M. T., Rajh, T. & Mićić, O. I. *J. phys. Chem.* **89**, 397 (1985).
11. Fojtik, A., Weller, H., Koch, U. & Henglein, A. *Ber. Bunsenges. Phys. Chem.* **88**, 969-977 (1984).
12. Gourley, P. L., Biefeld, R. M., Zipperian, T. E. & Wiczer, J. J. *Appl. Phys. Lett.* 983-985 (1984).
13. Ross, R. & Nozik, A. J. *J. appl. Phys.* **53**, 3813-3818 (1982).

Double seismic zone in Tonga

Hitoshi Kawakatsu

Department of Geophysics, Stanford University, Stanford, California 94305, USA

The clear evidence of a double seismic zone beneath Japan[1,2] has led seismologists to search for other such zones elsewhere. Because they have been found in few other areas[3-6], double seismic zones are thought to be rare and to depend strongly on a peculiar combination of external conditions (such as age of the descending slab, and the convergence rate)[7]. We report here a new double seismic zone which has been found beneath the Tonga arc[8], where the stress state in the subducting slab has been described as strongly down-dip compressional[7,9,10]. This discovery suggests that the double seismic zone is a general feature of subducting slabs and may be found in many other subduction zones.

A double seismic zone is a zone of double-planed activity of intermediate depth earthquakes in the subducting lithosphere, usually extending from 60 to 180 km depth (Fig. 1). The two planes are generally separated by ~40 km[1,2,11] at the shallow end and gradually merge at depth. The focal mechanisms of earthquakes in the upper and the lower planes tend to have compressional and tensional axes in the direction of the dip of the subducting slab, respectively[1]. Double seismic zones have been reported in Tohuku, Japan[1,2,12,13], Kuril and Kamchatka[3,14], eastern Aleutians[5,6] and Peru[4]. There have also been suggestions of double seismic zones in the central Aleutians[15] and Marianas[16], but the evidence is not conclusive[7,17,18].

Figure 2 shows a view of the general seismicity in the Tonga region with some tectonic features. The deeper portion (>300 km) of the slab has a high level of seismic activity and a down-dip compressional stress (or strain) state inferred from the earthquake focal mechanisms[10,19,20]. This has led to conclusions that the slab cannot penetrate into the lower mantle in this region[19,20]. It has also been suggested that the stress state of the intermediate depth range of the subducting slab under the Tonga arc is strongly down-dip compressional[7,9,10]. Isacks and Molnar[9] state that "a compressional stress is transmitted through nearly all parts of the slab". Even after the discovery of a clear double seismic zone in Japan, neither Billington[10] nor Fujita and Kanamori[7] hinted at the possiblity of a double seismic zone in the Tonga region, although they identified one event which shows down-dip tension at a depth of 186 km. However, a careful examination of the mechanisms and depths of earthquakes reveals that there are several down-dip tensional events in this region. They are located consistently deeper than and seawards of the down-dip compressional events, suggesting the presence of a double seismic zone.

Figure 3 clearly suggests the presence of a double seismic zone from a depth of ~60 km to ~200 km. This region (azimuth 109° to 116°) was chosen because both the geometry of the subducting plate (inferred from seismicity) and the focal mechanisms suggest that the deformation of the slab occurs in a simple two-dimensional manner[8]. North of azimuth 109° (~17.5° S), the end of the subduction zone results in hinge faulting, introducing more complicated stress and strain structure in the slab. South of azimuth 116° (~24.5 °S), the lateral bend of the slab near 26° S prevents a simple two-dimensional view of the subduction process.

Cross-sections with narrower azimuth ranges (every 1° along the strike of the trench)[8] including smaller events show that the down-dip compressional and tensional events are consistently located on the upper and the lower edge of the zone of seismicity, respectively, in every section. The result of relative relocation (Fig. 4) supports the presence of a double seismic zone. The down-dip tensional events in Figs 3 and 4 are consistently located seaward of and below the down-dip compressional events, exactly as expected for a double seismic zone.
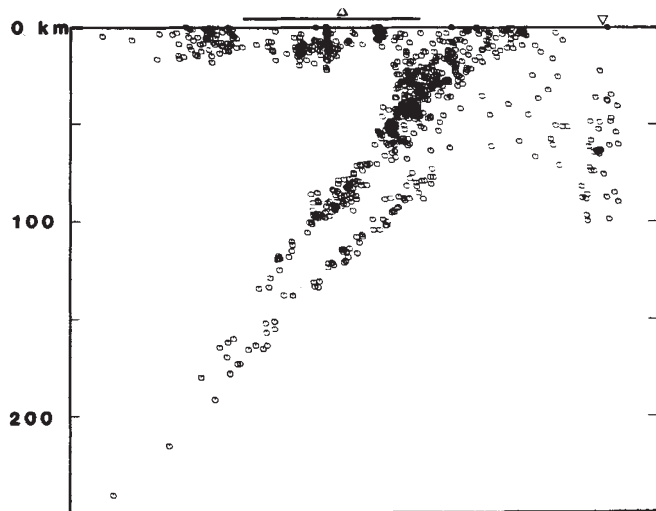
Fig. 1 Double seismic zone beneath the northern Honshu arc, Japan (after ref. 1). The precise determination of the microearthquake hypocentres using data from the seismic network of Tohoku University revealed a clear separation of two seismic zones. The figure is vertically exaggerated by a 2:1 ratio.
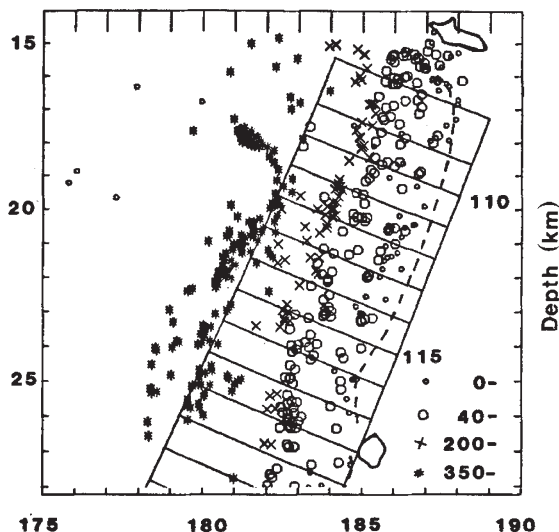

Fig. 2 Schematic view of the general seismicity of the Tonga subduction zone. The depth-constrained ISC events are plotted with tectonic features. The broken line represents the trench. The lines perpendicular to the trench are parts of the great circles which pass through the pole of the arc and the numbers denote the azimuth of the great circle measured clockwise from the north at the pole of the arc. The pole of the arc is located at 20.6° N, 102.8° E, so that the 100-km isodepth contour of Isacks and Barazangi[4] is 90° distant away from the pole. The two lines parallel to the strike of the trench are at the distances 87.5° and 92.5°.
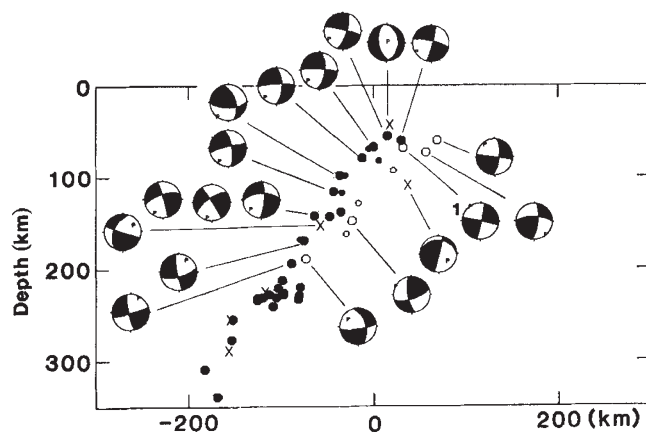

Fig. 3 Cross-section perpendicular to the tench. All the intermediate-depth (60 to 350 km) events occurring between azimuths 109° and 116° for which focal mechanisms are available, are plotted. ●, Down-dip compressional; O, down-dip tensional events; ×, events which are not either compressional or tensional. The small circles are events for which only the type of the mechanism can be determined[8]. The depths are all constrained by pP-P times reported with ISC. For the down-dip tensional events, depths are also checked by WWSSN seismograms. For events shallower than 200 km, the near side of the focal sphere is also plotted. Event 1: the depth (61 km)[23] of this large ($M_0 = 1.4 \times 10^{28}$ dyn cm)[23] normal fault event (22 June, 1977) is controversial[23]. The aftershock distribution[30] and the excitation of overtone surface waves (E. Okal, personal communication) seem to suggest that the faulting extended deeper than 100 km. Thus, the depth given here is probably the shallowest estimate.

What are the implications of this discovery of the double seismic zone beneath the Tonga arc? First, the double seismic zone is a rather persistent feature of subducting slabs. Tonga has the most active deep seismicity but the compressional strain (due either to inability of the slab to penetrate into the lower mantle[19,20] or to the strong viscous resistance to the subduction in the mesosphere[9]) transmitted from below 200 km depth cannot overprint and erase the pre-existing double seismic zone. On this basis, I predict that there is also a double seismic zone beneath the Izu–Bonin arc, even though it has active deep seismicity and down-dip compressional stresses. Furthermore, I speculate that a double seismic zone will be observed in most subduction zones (at least in those areas where both down-dip compressional and tensional events are already observed[7,9]). The observation of double seismic zones has been prevented by the lack of high-quality local networks in most subduction zones and the fact that the time span of reliable observations of earthquake focal mechanisms is too short. It has also been difficult to distinguish shallow (<80 km) down-dip tensional events from shallow-angle thrust faulting events, which are very common in subduction zones, without detailed wave-form analysis. This is because they have similar focal mechanisms and the reported depths (obtained by the International Seismology Centre (ISC) or by preliminary determination of epicentre) of shallow events are not reliable. A systematic analysis of these events, which can now be undertaken through the Global Digital Seismograph Network[21-23], will help to identify more down-dip tensional events.

Second, this discovery constrains possible mechanisms for the origin of the double seismic zone. It excludes geometrical sagging[24,25] as a possible mechanism since the strong down-dip compressional strain transmitted from below 200 km could easily overprint strain features caused solely by sagging. The simple geometrical unbending[15,16,26] with a brittle-plastic rheology suggested by Tsukahara[26] seems to be the best description of the physical mechanism of the double seismic zone.

Above a depth of ~60 km, oceanic lithosphere bends downwards when it subducts into the mantle. The fact that the subducting lithosphere appears to be straight in the mantle below a depth of ~200 km indicates that the lithosphere must unbend in a depth range from ~60 to ~200 km to become straight below a depth of ~200 km. A simple geometrical argument shows that the strain rate due to this unbending is of the order of 10^{-15} to 10^{-14} s^{-1} above a depth of ~100 km where most of unbending is taking place and is high enough to account for all the energy released by earthquakes of the double seismic zone[8]. Even below a depth of ~100 km where the slab appears to be straight, the

unbending strain rate can easily be of the order of 10^{-17} to 10^{-16} s^{-1} (an unbending strain rate of 10^{-17} s^{-1} of a 100-km thick slab, subducting 10 cm yr^{-1}, corresponds to a change of the dip angle of ~0.05°/100 km, which is impossible to detect from seismicity)[8]. On the other hand, the strain rate due to thermo-elasticity[27,28] (10^{-18} to 10^{-17} s^{-1})[28] is too low to be the main cause of the double seismic zone. Although all the other proposed mechanisms may contribute to its occurrence, the double seismic zone can be satisfactorily explained by the simple
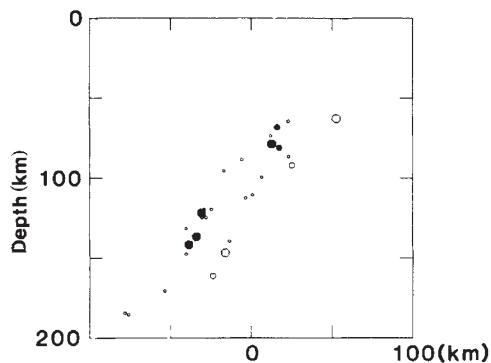
Fig. 4 To assign appropriate relative errors to the hypocentral parameters, a relative relocation was performed[8]. The method is similar to one used by Samowitz and Forsyth[16], except that here only depth constrained events are used. Data are selected from the ISC bulletin from 1971 to 1979 with the following conditions; pP-P constrained depths between 60 and 200 km; >30 P arrival observations. For the first iteration, all events are relocated with the depths fixed at the pP-P depths using the P-wave arrival times reported at stations between 30° and 100° distance and ISC locations as the starting guesses; 440 stations were used. After the first iteration, the stations which have arrivals from >10 earthquakes are selected and assigned station adjustments as a linear function of distance between stations and earthquakes by the least squares method. This leaves 113 stations. For the second iteration, travel times are first adjusted by using the station adjustments estimated in the first iteration. Each event was then relocated separately using only the arrivals from those 113 stations. The estimated relative errors (90% confidence intervals) are usually smaller than the largest circles. Symbols are as in Fig. 3. The smallest circles denote events for which no information about their focal mechanism is known. Although a clear separation of two seismic zones seems to exist, it could be coincidence[17]. Therefore, what is most important is that the down-dip compressional events are still always located above the down-dip tensional type events even after the relocation.

model of geometrical unbending. The cause of this unbending is uncertain and probably varies from place to place. For example, pressure due to mantle flow[29] (or equivalently, dynamical sagging[25]) or the weight of the slab itself can unbend the slab.

For a given magnitude of the strain rate, the distance between the two seismic zones depends strongly on the rheological properties and the thermal structure of the descending lithosphere[26]. Thus, as pointed out by Tsukahara[26], studies of the fine structure of double seismic zones in many areas will give important new information on the thermal and rheological properties of the subducting lithosphere[8].

I thank Bob Geller, Eric Peterson, Rick Schult and Norm Sleep for reviewing the manuscript. Comments by Drs Klaus Jacob and Bob Engdahl also improved the manuscript. This work was supported by NSF grants EAR82-18961 and EAR83-06555.

1. Hasegawa, A., Umino, N. & Takagi, A. *Tectonophysics* **47**, 43-58 (1978).
2. Hasegawa, A., Umino, N. & Takagi, A. *Geophys. J.R. astr. Soc.* **54**, 281-296 (1978).
3. Veith, K. F. thesis, Southern Methodist Univ., (1978).
4. Isacks, B. L. & Barazangi, M. *Island Arcs, Deep Sea Trenches and Back-Arc Basins* Vol. 1, 99-114 (American Geophysical Union, Washington DC, 1977).
5. Reyners, M. & Coles, K. J. *geophys. Res.* **87**, 356-366 (1982).
6. House, L. S. & Jacob, K. H. J. *geophys. Res.* **88**, 9347-9373 (1983).
7. Fujita, K. & Kanamori, H. *Geophys. J. R. astr. Soc.* **66**, 131-156 (1981).
8. Kawakatsu, H. thesis, Stanford Univ. (1985).
9. Isacks, B. L. & Molnar, P. *Nature* **223**, 1121-1124 (1969); *Rev. Geophys. Space Phys.* **9**, 103-174 (1971).
10. Billington, S. thesis, Cornell Univ. (1980).
11. Stefani, J. P., Geller, R. J. & Kroeger, G. C. J. *geophys. Res.* **87**, 323-328 (1982).
12. Yoshii, T. *Tectonophysics* **55**, 349-360 (1979).
13. Kawakatsu, H. & Seno, T. J. *geophys. Res.* **88**, 4215-4230 (1983).
14. Suzuki, S., Sasatani, T. & Motoya, Y. *Tectonophysics* **96**, 59-76 (1983).
15. Engdahl, E. R. & Scholz, C. H. *Geophys. Res. Lett.* **4**, 473-476 (1977).
16. Samowitz, I. & Forsyth, D. J. *geophys. Res.* **86**, 7013-7021 (1981).
17. Engdahl, E. R. & Fijita, K. J. *geophys. Res.* **86**, 7023-7024 (1981).
18. Topper, R. E. thesis, Univ. Colorado (1978).
19. Richter, F. M. J. *geophys. Res.* **84**, 6783-6795 (1979).
20. Giardini, D. & Woodhouse, J. H. *Nature* **307**, 505-509 (1984).
21. Dziewonski, A. M., Chou, T. A. & Woodhouse, J. H. J. *geophys. Res.* **86**, 2825-2852 (1981).
22. Dziewonski, A. M. & Woodhouse, J. H. J. *geophys. Res.* **88**, 3247-3271 (1983).
23. Giardini, D. *Geophys. J.R. astr. Soc.* **77**, 883-914 (1984).
24. Yoshii, T. *Kagaku* **47**, 170-176 (1977).
25. Sleep, N. H. J. *geophys. Res.* **84**, 4565-4571 (1979).
26. Tsukahara, H. J. *phys. Earth* **28**, 1-15 (1980).
27. Goto, K. & Hamaguchi, H. *Prog. Abstr. seism. Soc. Jap.* **2**, 36 (1978).
28. House, L. S. & Jacob, K. H. *Nature* **295**, 587-589 (1982).
29. Yokokura, T. *Tectonophysics* **77**, 35-62 (1981).
30. Silver, P. G. & Jordan, T. H. J. *geophys. Res.* **88**, 3273-3293 (1979).

The influence of subduction processes on the geochemistry of Japanese alkaline basalts

Eizo Nakamura*, Ian H. Campbell*† & Shen-su Sun†‡

* Department of Geology, University of Toronto, Toronto, Ontario, Canada M5S 1A1
† Research School of Earth Sciences, The Australian National University, GPO Box 4, Canberra, ACT 2601, Australia
‡ Division of Petrology and Geochemistry, Bureau of Mineral Resources, Geology and Geophysics, Canberra, ACT 2601, Australia

The composition of volcanic rocks erupted in complex plate tectonic settings can provide information on the nature of the underlying mantle. We show here that the geochemistry of alkali basalts from Japan and eastern Asia varies systematically with distance from the Japanese island-arc. Samples from northeastern Japan, relatively close to the Japan Trench, are enriched in K, Sr, Ba and Rb and depleted in Ta, Nb and Ti as compared with samples from southwestern Japan. Both sets show an island-arc influence on their composition, but alkali basalts from still further west (Korea and northeastern China) have chemistries which are indistinguishable from ocean island basalts. We suggest that the northeastern island-arc type of alkali basalts were derived from a 'normal' upper mantle source altered by fluids or melts released from the underlying subducted Pacific plate. The extent of this island-arc-related alteration decreases with distance from the trench.

Major and selected trace-element concentrations of 200 Tertiary to Recent alkali basalts were determined by a combination of X-ray fluorescence (XRF) and instrumental neutron activation analysis (INAA) using the method described by Barnes and Gorton[1]. Most of the samples analysed are nepheline normative and have the following characteristics: SiO_2 contents of less than 52 wt%, Ni contents of greater than 100 p.p.m., Cr contents greater than 150 p.p.m. and no detectable Eu anomalies. Samples with these characteristics are assumed to have retained their primitive chemistry. Olivine ± clinopyroxene fractionation may have produced a slight increase in the concentration of the incompatible elements in some samples but any change in ratios of these elements will be small.

Selected analyses are plotted on normalized abundance pattern (NAP) diagrams[2-5] (Fig. 1). These diagrams give the concentration of selected incompatible elements normalized to their concentration in the primitive mantle. The elements are arranged systematically in order of increasing incompatibility, with the most incompatible elements plotted on the left. Figure 1a gives NAPs for an average depleted mid-ocean ridge basalt[3,4], typical Hawaiian tholeiite[6] and alkali basalt[6], an average continental alkali basalt from Kenya[7], an average island-arc calc-alkaline basalt[4] and an average arc tholeiite[4]. Both island-arc rock types are characteristically enriched in K, Ba, Sr and Rb and depleted in Ta, Nb and Ti (weakly) relative to adjacent elements in the NAP diagram.

NAP diagrams for samples from Rishiri Island (northeastern Japan), southwestern Japan, Jejudo Island (Korea) and Datong (northeastern China) are plotted in Fig. 1b, c and d respectively. They can be divided into three types: an island-arc type enriched in K, Ba, Sr and Rb and depleted in Ta or Nb and Ti, a transitional type which shows a much weaker island-arc signature, and a normal type with a NAP typical of ocean island and continental alkali basalts. The island-arc type is confined